

Chromatic analysis of signals from a driver fatigue monitoring unit

Alex Koh, Gordon R Jones, Joe W Spencer and Ian Thomas

Centre of Intelligent Monitoring Systems (CIMS), Department of Electrical Engineering and Electronics, University of Liverpool, Brownlow Hill, Liverpool, L69 3GJ, UK

E-mail: alexkoh@gmail.com

Received 22 August 2006, in final form 23 November 2006

Published 24 January 2007

Online at stacks.iop.org/MST/18/747

Abstract

The problem of extracting quantified information from physiological and physical indicators of the fatigue level of a vehicle driver is addressed. A chromatic approach has been used for processing the physiological and physical outputs from a driver fatigue monitoring system, the physical indicator being in the form of gyroscopic signals produced by the lateral movements of a vehicle. Some preliminary results are presented which show how the chromatic signatures of the physiological and physical indicators can be used to identify fatigue thresholds and provide a more optimized estimate of tiredness.

Keywords: chromatic processing, driver fatigue, data analysis, advisory system, circadian rhythm, gyroscope, Gaussian, monitoring, physiological, tiredness

(Some figures in this article are in colour only in the electronic version)

1. Introduction

There is an increasing awareness of the role of fatigue in reducing the effectiveness of everyday tasks such as vehicle driving. Drowsy driving encompasses several aspects, including falling asleep while driving or simply not paying attention due to fatigue or lack of sleep. There is therefore a need to provide assistive monitoring for vehicle drivers to reduce possible accidents etc, which might be caused by over-fatigued driving. Such monitoring needs to take account of both person based attributes and physical technology based indicators of fatigue. Regarding the former there is a need to respect the human biological clock which determines the fatigueness and is called ‘circadian rhythm’ [1, 2].

There are a number of methods which have been proposed for monitoring signs of fatigue of an individual whilst driving a vehicle. These include the detection of the driver’s eye movement [3, 4], EEG (electroencephalogram) and EOG (electro-oculogram) [5, 6] etc. Whereas such methods are being tested at laboratory level, their reliability and implementation in real road situations remains to be proven and there are potential impediments such as cost and the complexity of the equipment to be addressed.

Another approach is to have a means which bridges the gap between physiological attributes and technical indicators. One such system is the ASTiD (advisory system for tired drivers) [7] system which is already in use on a number of vehicles. This system derives its output from the manner in which a vehicle is driven, inputted data by the driver and time of day related to circadian rhythm. The manner in which the vehicle is driven is determined from the vehicle response which is monitored in this system from the output of a gyroscope arranged to indicate the lateral movements of the vehicle. The research into fatigue and sleep shows that an early indicator of driver tiredness is given by a finite number of reactions resulting in particular corrective steering actions by the driver [2]. There is a need to better understand the capabilities of such systems with respect to their operation under real conditions. This contribution seeks to analyse the output signals from an ASTiD system. A chromatic processing technique [8, 9] is used for extracting relevant information from the complex data output relating to both the human physiological trends and those from the vehicle response.

It is shown that a chromatic transformation of the various data sets can enable significant signal patterns to be identified for providing an insight into a more rigorous approach for utilizing physiological and physical indications of fatigue.

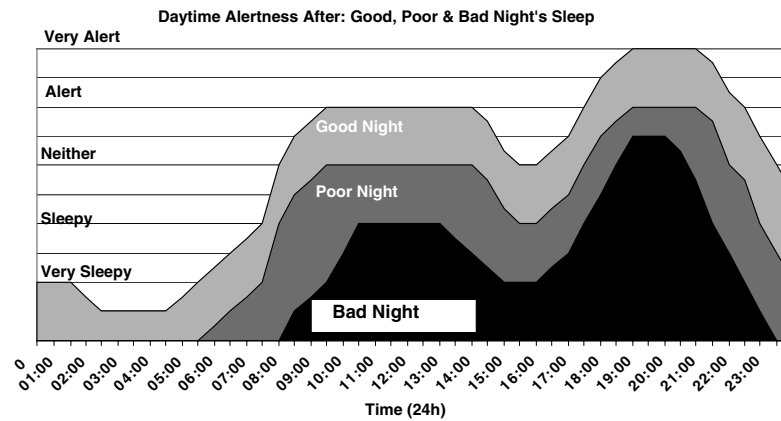


Figure 1. Circadian rhythm default plot for various sleeping conditions.

2. Test instrumentation

The instrumentation used consisted of an ASTiD (advisory system for tired drivers) [2]. This advisory system utilizes four sets of data which are

- the circadian rhythm representing diurnal variation in human tiredness;
- a driver's input about the quality of sleep before driving;
- a tiredness factor which increases with the continuous period of driving;
- a gyroscope output which indicates lateral movement of the vehicle being driven.

The circadian rhythm component (a) is derived from sleep research information from the University of Loughborough, Sleep Research Centre [1] and is embedded within a microprocessor in the ASTiD unit. Figure 1 shows the data for diurnal variation in alertness for different levels of sleep quality which is embedded in the ASTiD unit.

The quality of sleep judgement (b) 'good', 'poor', 'bad' is inputted into the ASTiD unit by the driver prior to commencing to drive. This chooses the appropriate circadian rhythm curve (figure 1) to be applied by the unit for that particular journey.

The quantification of the tiredness factor (c) is determined from studies on fatigue changes at the University of Loughborough and is again embedded within the microprocessor in the ASTiD unit. This yields the extent to which alertness decreases with the duration of driving and increases with period of resting from driving.

Whereas (a), (b), (c) are *a priori* determined physiological indicators approximately quantified, (d) is a direct measurement of a vehicle response to the driver's reactions. As such it forms the link between the physiological domain and real physical effects. This is achieved via a gyroscope embedded within the ASTiD unit which is appropriately mounted within the vehicle and firmly attached to the dashboard in such a manner that the gyroscope responds predominantly only to lateral movements of the vehicle (figure 2). The output of the gyroscope is mainly pulsatile in nature and is fed into the ASTiD embedded microprocessor. The number and extent of the pulsations are used in conjunction with the physiological indicators (a), (b), (c) to indicate the level of fatigue in order to alert when excessive thresholds are approached.



Figure 2. Shows the ASTiD system mounted on the dashboard of a vehicle.

The fatigue indications from each of the above components (a), (b), (c), (d) may be linearly summed to give an overall tiredness score (TS) given by

$$TS \cong C \cdot R(t) + D + (a_1 \delta(t)_1 - a_2 \delta(t)_2) + a_3 \sum_{t_w} P \quad (1)$$

where

- $CR(t)$ is the time-dependent circadian rhythm tiredness score (a) (figure 1);
- D is the driver estimate of sleep quality received (b) (figure 1);
- $a_1 \delta(t)_1$ is the time accumulating tiredness caused by continuous driving for a time interval $\delta(t)_1$, a_1 being constant (c);
- $a_2 \delta(t)_2$ is the time accumulating resting effect after driving cessation for a time interval $\delta(t)_2$, a_2 being constant (c);
- $a_3 \sum_{t_w} P$ is the sum of the amplitudes P of the output pulses from the gyroscope during the driving time window t_w and a_3 is a numerical constant;
- t is time.

When the tiredness score (TS) exceeds a threshold predetermined from Sleep Research studies [1] the driver is alerted. The system at present yields a fail safe threshold with a good margin. A more precise estimate of the approach to the fatigue threshold might be achieved by better correlation of the data from the fatigue indicators (a), (b), (c) above.

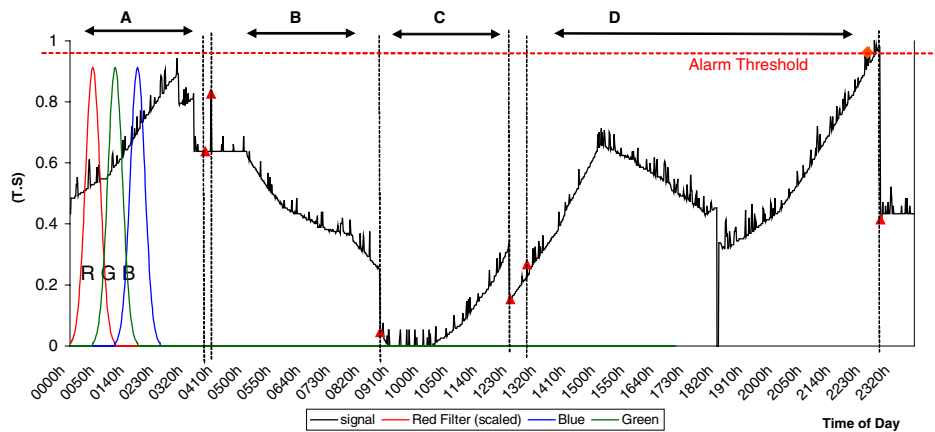


Figure 3. Typical output of the ASTiD system from a typical 24 h period test with several changes of drivers. (A, B, C, D different driver and shift periods.)

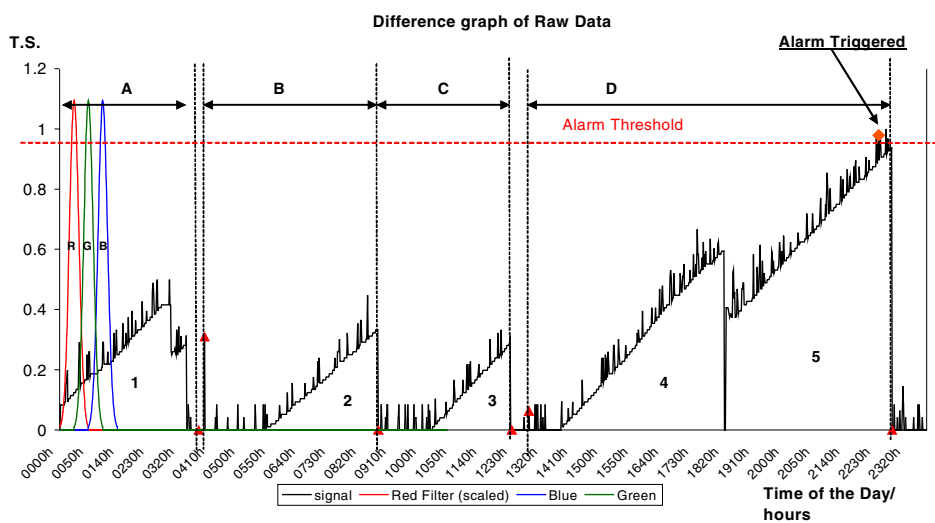


Figure 4. Difference graph of the raw data (figure 3). (Difference graph = raw data – circadian rhythm.) (A, B, C, D—drivers. 1, 2, 3, 4, 5—sectorial regions of increasing tiredness.)

3. Experimental tests

Two different sets of tests have been performed. The first set was with a commercial vehicle in routine use and driven by professional drivers with an ASTiD unit operating routinely. The second set was with a vehicle in which the output of the ASTiD gyroscope was monitored directly.

3.1. ASTiD unit output test

Experimental tests were performed with the ASTiD unit appropriately mounted on the dashboard of a commercial vehicle (figure 2) which was in routine use on normal roads, and when there were changes of drivers, rest periods and extensive road driving.

During such tests the overall output of the ASTiD unit was recorded as a function of time along with notes of major events such as time of start of driving, rest period, change of driver etc. The ASTiD unit also had inputted each driver's estimate of the quality sleep prior to driving. Also the outputs of the gyroscope as a function of time could be accessed retrospectively from the microprocessor embedded within the ASTiD unit.

Consequently test data could be retrieved after each test in the form of the time variation of the overall output of the ASTiD unit based upon the sum of the circadian rhythm curve appropriate to each driver, the fatigue increase during a driving session and the raw gyroscope output (equation (1)).

3.2. Gyroscope output tests

Tests were also undertaken whereby only the output of the gyroscope appropriately mounted on the dashboard of a vehicle was recorded directly in the absence of the circadian rhythm (a) and accumulative fatigue ((b) and (c)) outputs. During these tests, records of detailed observations of different driving conditions (e.g. different speeds, road conditions etc) were obtained by a passenger in the vehicle over a limited time interval (e.g. 6 min). During such tests the data sampling rate was 32 Hz.

4. Experimental results

Results from a typical 24 h test with driver changes obtained with the ASTiD system (figure 2) are shown in figures 3, and figure 4 corresponding respectively to the overall tiredness

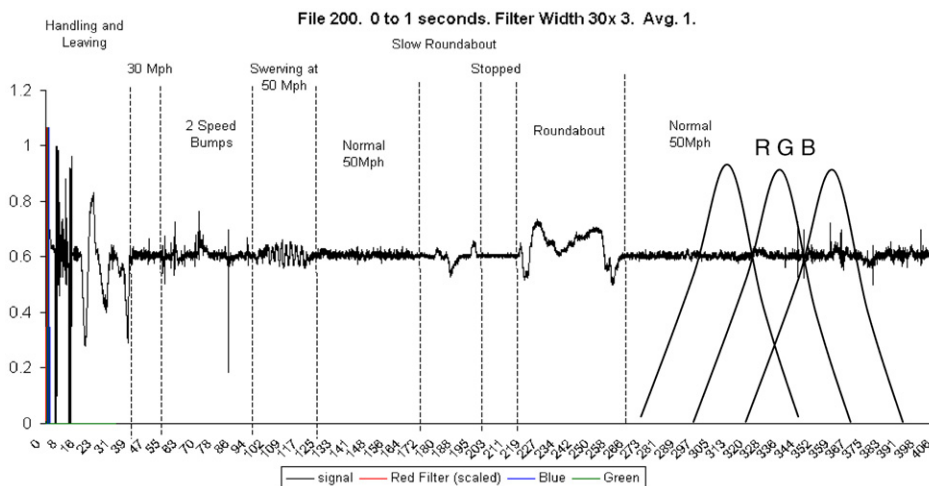


Figure 5. Gyroscope output showing different signals associated with various driving features.

score (equation (1)) and the tiredness score without the circadian contribution. More detailed results for a gyroscope test are shown in figure 5.

4.1. Overall output data

The overall output from the ASTiD unit (figure 3) shows a complex variation of TS with time. There are relatively slow variations due to the circadian rhythm ((a) section 2) combined with the continuous driving factor (b). There are also effects due to a total of four driver changes which occurred during different shift periods namely 03.30 (A), 08.46 (B), 12.30 (C) and 22.55 (D) hours. A change of driver is accompanied by the system resetting itself to the relevant point on the circadian rhythm. Likewise a driver resting reduces the tiredness score.

Superimposed upon the slower TS variations are short duration pulses which are the rapid response of the gyroscope to driver-induced lateral movement of the vehicle.

Based upon the Sleep Research conclusions of the University of Loughborough [1] a TS of 0.95 is regarded as the threshold for an unacceptably high tiredness level. This is shown as a dashed line in figure 3. In practice when $TS \geq 0.95$ an alarm is triggered to advise the driver to stop driving.

The circadian rhythm component (figure 1, (a), (b), section 2) may be removed from the overall TS in order to observe the effects of the other factors, i.e. fatigue increase with duration of driving ((c) section 2) and gyroscope output ((d) section 2).

The circadian rhythm [1] shows a daily cyclical pattern (figure 1) with a maximum tiredness at night time (03.00–05.00 hours) followed by a maximum period of awakesness (09.00–11.00 hours), a further tiredness peak (15.00 hours) and a wakeful period (17.30–20.00 hours). The absolute level of the circadian rhythm decreases with the quality of sleep leading to the three curves of figure 1.

Subtraction of the circadian rhythm component from the overall ASTiD output signal (equation (1)) leads to the time varying difference TS shown in figure 4. This graph shows that with fresh drivers (A, B, C, D figure 3) the tiredness score resets to zero. During the final phase of the day (sector D figure 3), there was no driver change therefore the tiredness

score remained accumulative for prolonged periods (approx. 10 h) of driving with eventually the alarm being triggered at 22.33 hours.

Five time sectors of increasing tiredness can be identified in figure 4 which are designated by 1, 2, 3, 4 and 5. Each refers to a different driver apart from 4 and 5 which refers to a single driver D who reset at 18.20 hours so reducing the tiredness level (from 0.6 to 0.4) yielding the two regions of tiredness 4 and 5.

4.2. Gyroscope output data

Results for the time variation of only the output from the gyroscope during a test when detailed observations of driving conditions were made are shown in figure 5. The results which are typical of those obtained from such tests covered a total period of 6 min. The vehicle was deliberately driven through a number of phases (figure 5) which included the following:

- (1) handling and leaving a stationary state;
- (2) travelling at 30 mph;
- (3) traversing two speed bumps;
- (4) deliberate swerving for 20 s to simulate swerving due to fatigue;
- (5) travelling at 50 mph;
- (6) slow negotiating of a roundabout;
- (7) vehicle stationary;
- (8) more rapid negotiation of a roundabout (two circulations);
- (9) travelling at 50 mph.

5. Analysis of results

The results given in figures 3, 4 and 5 show a number of features which are qualitatively distinguishable but warrant being examined quantitatively. For example discrimination of the 50 mph swerving detected by the gyroscope (figure 5) from the other driving artefacts would be particularly useful since it is generally recognized [1, 2] that a fatigued driver tends to drift off the road and swerve back as consciousness is regained. In order to explore the possibility of such quantified discrimination, chromatic techniques [8, 9] have been employed.

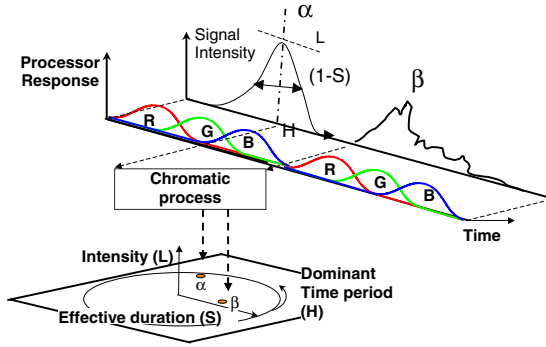


Figure 6. Time-dependent chromaticity showing time varying signals (α , β) during different times, each addressed by the chromatic processors (R , G , B) to yield H , L , S values. Each signal is replaced by a single point on the chromatic polar diagram.

5.1. Chromatic methodology

The deployment of chromatic processing was originally used with respect to optical wavelength [8] but subsequently it has been used for other parameters [9] and purposes [10]. In this application it is time-based chromatic processing which is deployed.

The time varying signal is addressed by three time based non-orthogonal filters R , G , B each of equal width and spanning a predetermined period (figure 6). The R , G , B outputs yield the chromatic parameters H , L and S defined by (equations (2)–(4) respectively), which in the present context have the following meaning. H represents the dominant signal time period, L is the nominal signal strength and S is the effective time duration of the signal within the monitored time window.

$$H = \left\{ \begin{array}{l} 60 \frac{G - B}{\max(R, G, B) - \min(R, G, B)}, \quad \text{if } R = \max \\ 60 \left[2 + \frac{B - R}{\max(R, G, B) - \min(R, G, B)} \right], \quad \text{if } G = \max \\ 60 \left[4 + \frac{R - G}{\max(R, G, B) - \min(R, G, B)} \right], \quad \text{if } B = \max \end{array} \right\} \quad (2)$$

$$L = \frac{\max(R, G, B) + \min(R, G, B)}{2} \quad (3)$$

$$S = \left\{ \begin{array}{l} \frac{\max(R, G, B) - \min(R, G, B)}{\max(R, G, B) + \min(R, G, B)}, \quad \text{if } L \leq 0.5 \\ \frac{\max(R, G, B) - \min(R, G, B)}{2 - \max(R, G, B) - \min(R, G, B)}, \quad \text{otherwise} \end{array} \right\} \quad (4)$$

The H , L , S parameters may be displayed on a polar plot with $\theta \equiv H$, $r \equiv S$, $z \equiv L$, as shown in figure 6. Signal α (figure 6) is a simple Gaussian pulse in time which serves as an aide to indicate the physical meaning of H , L , S . In practice the three filters are time stepped using an appropriate step width relative to the filter width. Figure 6 shows how the Gaussian signal α is followed by a more complex signal envelope β and addressed by the three chromatic filters R , G , B n time steps later.

The chromatic coordinates of the point corresponding to β have a lower S value (more broadly spread signal) with its dominant time earlier (H lower) than α . This example shows how various signals can be discriminated in terms of their chromatic coordinates.

5.2. Chromatic processing of fatigue signals

The chromatic processing approach described in section 4.1 may be applied to the analysis of the time varying signals shown in figures 3–5. Also shown in the figures are R , G , B filters in time-domain mode. Each of the R , G , B filters of figures 3 and 4 has a width 75 min and were time stepped in increments of 1 min over the entire signal duration. The R , G , B filters of figure 5 each had a width 30 (0.9 s) and were time stepped with a step width of 0.03 s. Values of the chromatic parameters H , L , S equations (2)–(4) were obtained for each time window.

These H , L , S values may then be displayed on polar plots of H – L or H – S (H is the azimuthal angle and L , S are the radii, respectively) to highlight features of interest from the raw data. The choice between using H – L or H – S depends upon the information being sought.

5.2.1. Overall output signal. Applying the chromatic analysis to the overall data of figure 3 yields the H – L polar diagram of figure 7. Data for each driver are designated by A–D as shown in figure 3. An alarm which was triggered at 22.33 hours (figure 3) has H , L coordinates 210, 0.8. Arrows show the tiredness progression.

The results show loci for the various drivers with many convolutes on the $H \sim 30^\circ$ – 210° axes. Within the second quadrant (90° – 180°) there are three arcs apparent (corresponding to drivers A, B, D) whilst within the fourth quadrant (270° – 360°) there is only a single arc apparent (driver C).

5.2.2. Difference data analysis. Applying the chromatic analysis to the difference data of figure 4 yields the H – L polar diagram of figure 8. In this case the five different time stages of figure 4 (1–5) are distinguished by different symbols. The 22.33 hour alarm has H – L polar coordinates 210, 0.8 which are identical to the figure 7 values.

The results show a number of loci in the sector 90° – 180° the length of whose radii are related to the magnitude of the tiredness factor of figure 4. The effect of a driver resting (separating region 4, 5, figure 4) appears as an excursion into the quadrant 270° – 360° figure 8. The most rapid increase in tiredness score appears as a radial increase in L along the 210° radius.

5.2.3. Gyroscope data analysis. Chromatic analysis of the gyroscope output signal (figure 5) leads to the H – S polar diagram shown in figure 9. The nine different manoeuvres ((1)–(9) section 4.2, figure 5) are designated on figure 9 by different symbols.

Most of the manoeuvres appear as ellipses with major axes inclined along the $H \sim 30^\circ$ – 210° axis and with a minor axis value of $S \sim 0.2$. However, the swerving action (curve 4, figure 9) is circular with a radius $S \sim 0.3$ – 0.4 .

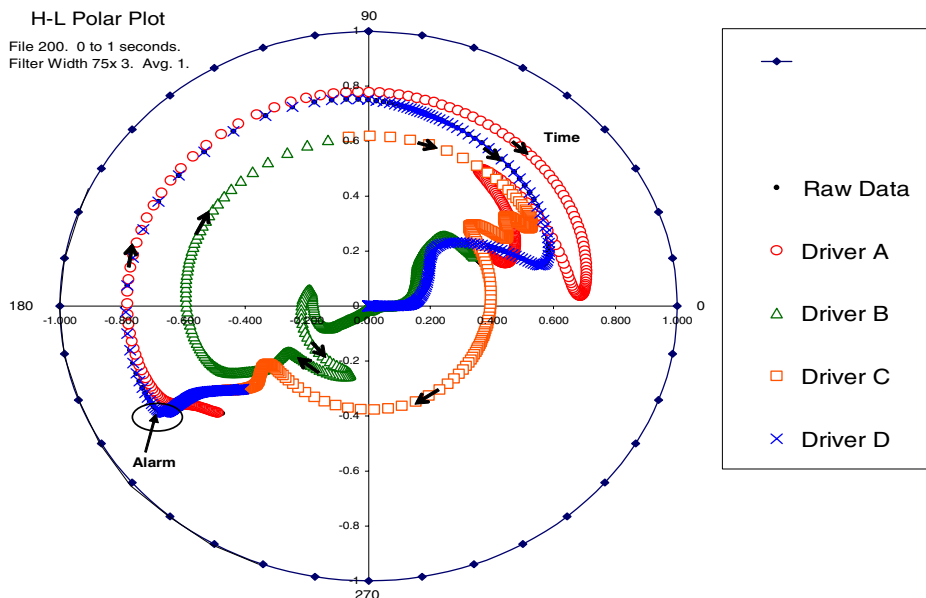


Figure 7. Chromatic polar-diagram $H-L$ for the overall output signal of figure 3. (Different symbols correspond to various drivers A–D, figure 3.)

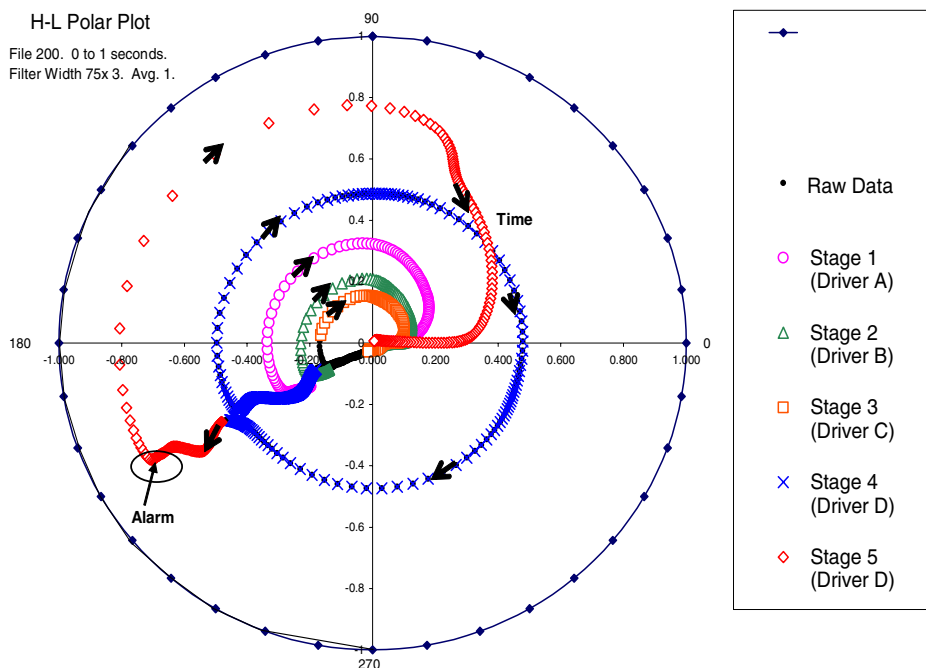


Figure 8. Chromatic polar-diagram of $H-L$ for the difference data of figure 4. (Different symbols indicate different stages of figure 4.)

6. Discussion of results

The results of the chromatic analysis presented in section 5 as $H-L$ and $H-S$ polar diagrams may be considered in terms of the extent to which various features are associated with different manoeuvres. The physiological components are considered first (figures 7 and 8) before discussing the gyroscope output figure 9 and the combined information.

6.1. Physiological results

The chromaticity transformed physiological trends (figures 7 and 8) may be interpreted by comparison with the raw time-

domain data of figures 3 and 4. The $H-L$ polar diagram of figure 8 in conjunction with the difference graph figure 4 leads to the following conclusions:

- for no driver activity $L \sim 0, S \sim 0$;
- the locus of points on the $H-L$ diagram is sequenced in a clockwise direction (arrows);
- tiredness reduction (due to resting or a change of driver) leads to decreasing L values in quadrant 1 ($H \sim 0^\circ-90^\circ$);
- when the tiredness reduction does not lead to a complete recovery but is interrupted by a return to tiredness increasing (stages 4 and 5 in figure 4), the $H-L$ locus

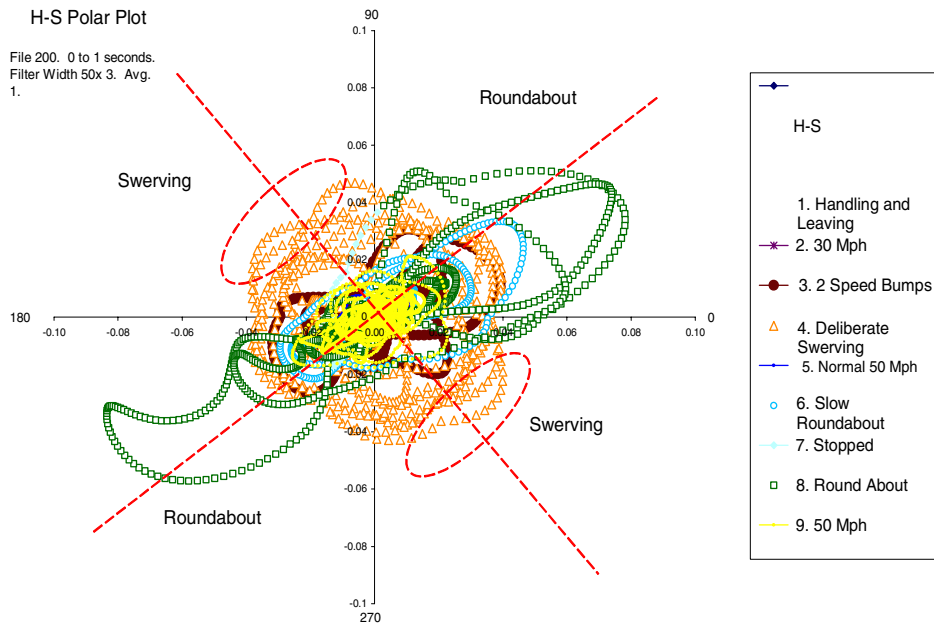


Figure 9. H - S polar diagram of the gyroscope output of figure 5. (Different symbols indicate different manoeuvres of figure 5.)

is within the fourth quadrant ($H \sim 270^\circ$ - 360°) (figure 8) at approximately constant L ;

- tiredness increasing is reflected in L increasing at constant H ($\sim 210^\circ$) in quadrant 3 (figure 8);
- the magnitudes of the tiredness peaks in stages 1, 2, 3, 4, 5 (figure 4) are reflected by the L values of the arc in the second quadrant ($H = 90^\circ$ - 180°) (figure 8).

The chromatically processed results for the combination of circadian rhythm and tiredness factor (figure 7) show similar trends to the difference results of figure 8. However the circadian rhythm component can contribute significantly in moving some trajectories further or closer to the critical threshold boundary. For example driver A's locus has a relatively low value of $L \sim 0.37$ in figure 8 but a higher value of 0.8 in figure 7.

These observations enable the implications of various sectors of the chromatically processed H - L signals to be appreciated as shown schematically in figure 10. The first quadrant of figure 10 corresponds to a progressive reduction in tiredness (i.e. decreasing tiredness, figure 4). The second quadrant of figure 10 corresponds to the tiredness level having passed through a peak. The third quadrant accommodates increasing tiredness trends whilst the fourth quadrant indicates a change in tiredness trends from initially decreasing (due to resting) to increasing (restart of driving).

Thus in general the lightness level L (radius in figure 10) represents the extent of tiredness whilst the H value is indicative of whether tiredness increases or decreases. A threshold for critical tiredness level may therefore be defined (figure 10) above which an alarm may be initiated.

6.2. Gyroscope results

In the case of the gyroscope results (figures 5 and 9), it is the H - S rather than the H - L chromatic map which provides a discrimination capability. Under 'normal' driving conditions

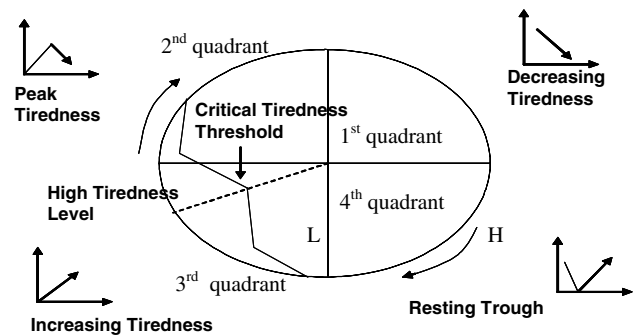


Figure 10. H - L polar diagram showing the critical tiredness threshold.

the H - S chromatically transformed data cluster about the origin. Manoeuvring roundabouts leads to lobes being formed along the 30° and 310° axis on the polar diagram (figure 8). However, the swerving motion in figure 5 produced more pronounced lobes within the second and third quartiles of the H - S diagram, where previously there had been only lower S levels. This implies that the time variation of the swerve signal (figure 5) is more regular than the other manoeuvre signals.

6.3. Combination of physiological and gyroscope signals

The results of figures 8 and 9 show that in the chromatic domain

- the physiological critical tiredness threshold has polar coordinates ($L > 0.8$, $180^\circ < H < 270^\circ$);
- tiredness induced swerves (gyroscope signals) has polar coordinates ($S \geq 0.04$, $H = 120^\circ$, 300°).

Thus whereas physiologically it is signal strength (L) combined with the L trend with respect to H which indicates the tiredness threshold, physically (gyroscope) it is the degree of monochromaticity ($1 - S$) at a particular part of the signal

(H) which is indicative of tiredness. Consequently summing the physiological and physical signal strengths (equation (1)) is rigorously inappropriate but provides a fail safe margin by taking all gyroscope pulses into account.

If a better optimized tiredness estimate is to be achieved, the difference in the chromatic domain physiological and physical indicators (section 6.3) needs to be respected implying that each needs to be treated separately and the two results then cross-correlated.

For the physiological case, the tiredness score may be expressed in chromatic terms as

$$(TS)_p = L(H) \quad (5)$$

with the critical tiredness threshold as

$$(TS)_{pT} = 0.8 \quad (180^\circ < H < 270^\circ). \quad (6)$$

In the physical case (gyroscope), it is the occurrence of a particular type of pulse defined by ($S \geq 0.4$, $H = 120^\circ$, 300°) which is indicative of tiredness. Sleep research [1, 2] suggests that it is the number of such swerves within a given time window which is indicative of the degree of tiredness. Consequently, the physically based tiredness score ($(TS)_g$) may be related to the occurrence of the identifying signal $S_g(S, H)$ by

$$(TS)_g = \sum S_g(\geq 0.4; 120^\circ/300^\circ) \quad (7)$$

with a critical physical tiredness threshold as

$$(TS)_{gT} = N_t \quad (8)$$

where N_t is an empirically determined number of the particular pulses detected in a given time window t to be unacceptable.

For the two extreme dominating cases

- physiological indicators,
- physical (gyroscope) signals,

the tiredness score compared to the relevant threshold $[(TS)/(TS)_T]$ is conveniently given by equations (5)–(8) respectively.

For the cases when physiological and physical indicators both contribute, it is anticipated that the tiredness scores from equations (5) and (7) would correlate to indicate similar rates of increase of tiredness and approaches to each of the two critical tiredness thresholds as given by equations (6) and (8). Otherwise the most critical indicator might be adopted pending further experimentation and the possible use of additional chromatically based prognosis as used by Zhang *et al* [11].

7. Conclusions

It has been shown how time-domain chromatic processing may be applied to different types of signals from a driver fatigue monitoring system. Data are transformed into H – L or H – S chromatic maps on which signatures for different levels and trends of fatigue can be observed.

Physiologically based fatigue indicators have been shown to be distinguishable on an H – L polar diagram. Swerving motion associated with the onset of high levels of fatigue as detected by a gyroscope has been shown to be distinguishable from other types of lateral motions on an H – S polar diagram.

This suggests that adding the magnitudes of the physiological and physical signals equation (1) is an over simplification but one which provides a high fail safe margin of fatigue estimation since it considers all rather than only some gyroscope outputs as significant.

In order to better optimize fatigue estimation, it is suggested that the physiological and physical indicators are treated separately in the chromatic domain pending the availability of additional test data to enable chromatic probability methods [11] to be invoked. Further tests are also needed to establish the extent to which swerve signals are discernible under other operating conditions (e.g. various drivers, vehicles, weather conditions etc). Such tests are currently ongoing.

Acknowledgments

The authors appreciate the provision of an ASTiD system and test data by Pernix which enabled the present work to be undertaken. Financial support provided by the EU via the IMS 2000 project is acknowledged. Discussions with Professor J Horne and Dr L A Reyner of the Sleep Research Unit of Loughborough University are also much appreciated as are the efforts of Ms S Kallio in producing this manuscript.

References

- [1] Horne J A and Reyner L A 1995 Sleep related vehicle accidents *Br. Med. J.* **310** 565–7
- [2] Reyner L A and Horne J A 1998 Falling asleep whilst driving: are drivers aware of prior sleepiness? *Int. J. Legal Med.* **111** 120–3
- [3] Johns M W 2003 The amplitude–velocity ratio of blinks: a new method for monitoring drowsiness *Sleep (Suppl.)* **26** A51–2
- [4] Leder R S, Stampi C and Webster J G 1996 Blink size and lid velocity from ambulatory subjects: an analog, retroreflective eyelid sensor *J. Sleep Res.* (Suppl. 1) 121
- [5] Held C M, Causa L, Estevez P, Perez C, Garrido M, Algarin C and Peirano P 2004 Dual approach for automated sleep spindles detection within EEG background activity in infant polysomnograms *26th Annual Int. Conf. Eng. Medicine and Biology Society (1–5 Sept)* vol 1 pp 566–9
- [6] Peiris M T R, Jones R D, Davidson P R, Carroll G J, Parkin P J, Signal T L, Van DenBerg M and Bones P J 2005 Identification of vigilance lapses using EEG/EOG by expert human raters *27th Annual Int. Conf. Eng. in Medicine and Biology Society (01–04 Sept.)* pp 5735–7
- [7] <http://www.pernix.co.uk/>
- [8] Jones G R and Russell P C 1993 Chromatic modulation based metrology *Pure Appl. Opt.* **2** 87–110
- [9] Jones G R, Russell P C, Vourdas A, Cosgrave J, Stergioulas L and Haber R 2000 The Gabor transform basis of chromatic monitoring *Meas. Sci. Technol.* **11** 489–98
- [10] Brazier K J, Deakin A G, Cooke R D, Russell P C and Jones G R 2001 Colour space mining for industrial monitoring *Data Mining for Design and Manufacturing (Massive Computing Series vol 3)* ed D Braha (Dordrecht, The Netherlands: Kluwer)
- [11] Zhang J, Jones G R, Deakin A G and Spencer J W 2005 Chromatic processing of DGA data produced by partial discharges for the prognosis of HV transformer behaviour *Meas. Sci. Technol.* **16** 556–61